

## Fracture Intensity Distributions during Compression of Puffed Corn Meal Extrudates: Method for Quantifying Fracturability

A.H. BARRETT, S. ROSENBERG, and E.W. ROSS

### ABSTRACT

The distribution of fracture intensities occurring during compression of puffed corn meal extrudates was described using an exponential function, and parameters from that analysis were used as fracturability indices. Since "jagged" or oscillating stress-strain functions are typical for porous and brittle materials, fracture intensities were determined by measuring the abrupt, sequential reductions in stress produced during compression. Both distribution exponent and cumulative fracture stress correlated strongly with fracturability measured by other techniques, including fractal and Fourier analysis of stress-strain functions. Distribution parameters also indicated textural differences due to process parameters (structural modification through addition of different levels of sucrose) and storage conditions (equilibration at various relative humidities).

**Key Words:** corn meal, extrudates, fracturability, compression

### INTRODUCTION

FRACTURABILITY is an important textural property of many widely consumed foods. "Crunchy" products, which are often porous and brittle, constitute a large category of breakfast cereals and snack foods. Many of these products are formed by high-temperature, short-time extrusion, which effectively puffs the material into a cellular and open structure. Texture in these products arises from an incremental and progressive fracturing of cell wall components in response to deformation. During mastication such fracturing gives rise to specific sensory perceptions such as crunchiness.

Fracturability is a complex mechanism often requiring sophisticated instrumentation and mathematical techniques to evaluate. Previously, texture in extrudates has been evaluated by force-deformation analysis and determination of elastic properties such as modulus (Smith, 1992; Halek et al., 1989; Launey and Lisch, 1985) or single-parameter failure properties such as breaking stress (Lai et al., 1989; Faubion and Hosenev, 1982). More recently, fracturability has been described by analysis of extended strain compression functions, in which repeated fracturing results in oscillating stress levels—giving rise to "jagged" stress-strain relationships. This property was described in terms of Fourier and fractal analysis by Barrett et al. (1992) and Rhode et al. (1993), and used in Symmetrized Dot Patterns (SDP) plots by Peleg and Normand (1992). In those studies Fourier analysis provided power spectra that indicated frequencies of fracturing, and fractal analysis provided a numerical measurement of the overall roughness of the stress-strain function; SDP plots were used to visually determine differences in the failure patterns of foods. Fracturability parameters from fractal and Fourier analysis, respectively fractal dimension and average intensity within specific frequency ranges of the power spectrum, correlated with extrudate structure and sensory texture (Barrett et al., 1994). One of the additives these authors employed to vary cell structure was sucrose, which has been reported to alter extrudate expansion and/or mechanical properties (Hsieh et al., 1990; Ryu et al., 1993; Sopade and Le Grys, 1991).

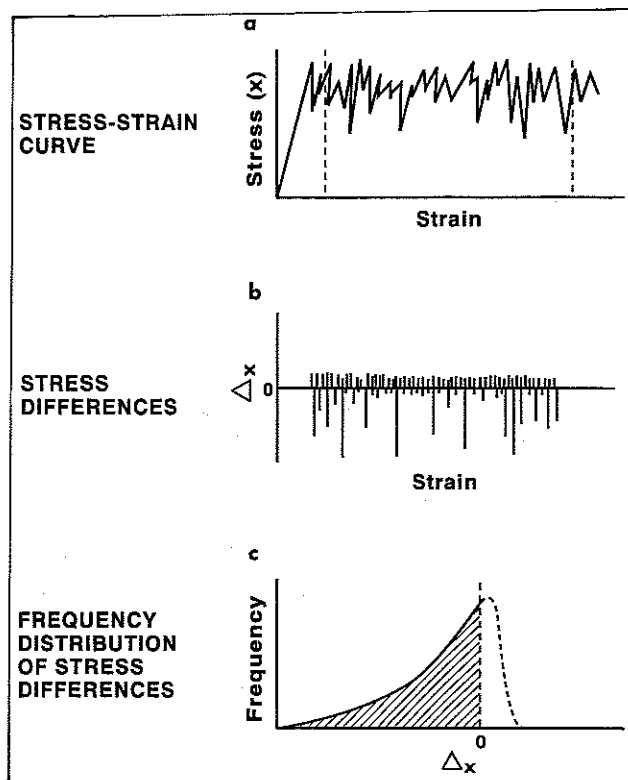


Fig. 1.—Procedural sequence for determining fracture intensity (stress difference) distributions. X refers to stress.

Our objective was to describe quantitatively the distribution of fracture intensities that occurs during compression of extrudates and to use parameters from those distributions as fracturability indices. Such a methodology employs mathematical procedures that are readily available in basic spreadsheet programs. Extrudate structures and mechanical properties were varied through addition of different levels of sucrose; textural changes in the samples were also produced by storage at elevated humidity. Parameters from fracture intensity distributions were tested for correlation with fracturability parameters from fractal and Fourier analysis.

### MATERIALS & METHODS

SIX BATCHES OF CORN MEAL (Lincoln Grain Co.) extrudates with sucrose contents of 0, 2, 4, 6, 8, and 10% were produced on a Werner and Pfleiderer ZSK-30 twin screw extruder. For each batch, a feed rate of 27 kg/hr, a moisture content of 15%, a six-zone temperature profile of 38-38-116-116-138-138°C and a 4 mm die were used. Extrudates were freeze dried after extrusion. Samples for high-humidity tests were equilibrated over saturated solutions of KCO<sub>3</sub> (43% RH) and NaCl (75% RH) for 48 hr.

#### Compression

Extrudates were sliced into 12 mm thick discs and compressed to 50% strain on a Texture Technologies TX2 texture press interfaced with a Zenith 286 computer. Before compression, three caliper measurements were taken of the diameter of each specimen and averaged. A compression rate of 0.2 mm/s and force-distance data acquisition

Authors Barrett and Rosenberg are with the Advanced Foods Branch, Sustainability Directorate, U.S. Army Natick RD&E Center, Natick, MA 01760-5018. Author Ross is with the Dept. of Mathematical Sciences, Worcester Polytechnic Institute, Worcester, MA.

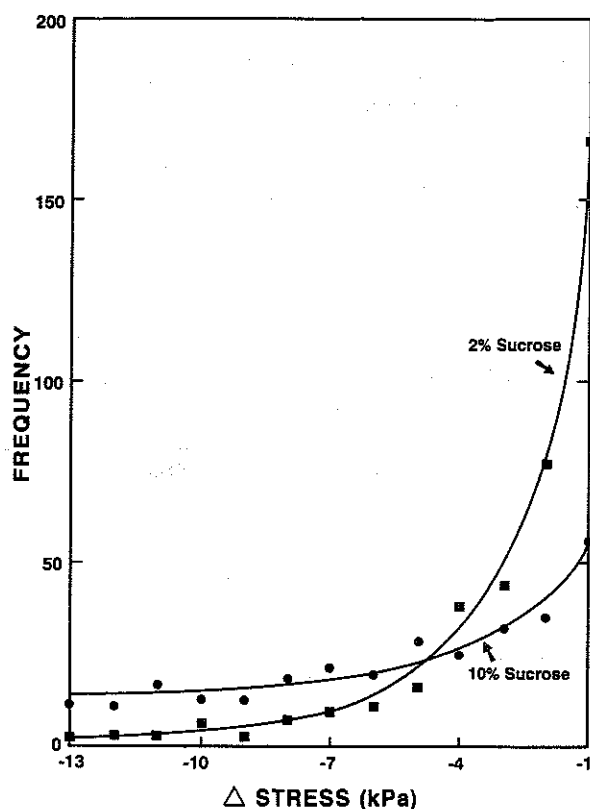


Fig. 2.—Fracture intensity distributions (6 replicates combined) for samples containing 2% sucrose and 10% sucrose.

Table 1—Fracture intensity distribution parameters and extrudate expansion

Sucrose content	Exponential distribution parameters and fit			Extrudate expansion ratio
	b (Exponent)	C (Coefficient)	r <sup>2</sup>	
0	0.352	10.5	0.87	30.8
2	0.490	15.5	0.90	28.9
4	0.307	10.6	0.95	28.9
6	0.363	11.6	0.86	26.8
8	0.209	7.0	0.86	24.5
10	0.093	3.0	0.78	16.8

rate of 12.5 pts/sec were used. The middle 2/3 of each compression curve (8–42% strain region) was saved for analysis. Samples were compressed at room temperature (25°C).

#### Cumulative fracture stress measurement

Force-distance data files were imported into a Minitab<sup>TM</sup> statistical program, converted to stress-strain values and analyzed in the procedural sequence shown in Fig. 1. Incremental changes in stress were determined by differences in the data according to the formula:

$$\Delta x_i = x_i - x_{i-1}$$

In the difference data file negative  $\Delta x_i$  values indicate reductions in stress, or fractures, whereas positive values are incremental increases in stress due to compression (Fig. 1b). A frequency distribution of fracture intensities (negative  $\Delta x_i$  values) was constructed from the difference data, (Fig. 1c) and numerically summed to determine the cumulative fracture stress. Six replicates of each sample were compressed and the summed fracture intensities averaged.

#### Fracture intensity distribution analysis

The six frequency distribution replicates for each sample were combined and then truncated by removing the largest 5% of the stress

reductions (since the distributions were long-tailed). This distribution was divided by 6 to yield an "average" distribution per compression and fitted to the exponential form

$$y = \text{frequency} = Ce^{(b\Delta x)}$$

where C and b are parameters of the distribution. The exponent, b, indicates the relative preponderance of low intensity vs high intensity fractures; the coefficient, C, indicates the number of fractures below a minimum observable non-zero stress reduction.

The distribution tail (high intensity fracture range) was investigated by the extreme value procedure proposed by Gumbel (1958). This method tested whether the largest fracture intensities were consistent with the main body of the exponential distribution or arose from an entirely different distribution (suggesting a different mechanism for low and high fracture intensities). The following relationships were used: if U is an exponential random variable with density function  $be^{bU}$ , and  $L_n(n)$  is the largest value of U in a sample of size n from that variable, then

$$\overline{L_n(n)} = \text{mean of } L_n(n) = \frac{1}{b} \sum_{k=1}^n \frac{1}{k}$$

$$\sigma_{L_n(n)}^2 = \text{variance of } L_n(n) = \frac{1}{b^2} \sum_{k=1}^n \frac{1}{k^2}$$

if  $n \gg 1$ , then

$$\overline{L_n(n)} \approx (\ln(n) + 0.577)$$

$$\sigma_{L_n(n)}^2 \approx \pi^2/(6b^2)$$

if the most extreme value satisfies the inequalities

$$\overline{L_n(n)} - 2\sigma_{L_n(n)} \leq L_n(n) \leq \overline{L_n(n)} + 2\sigma_{L_n(n)}$$

then it can be concluded (with  $\approx 95\%$  confidence) that the extreme value does not conflict with the exponential model, i.e., the mechanism governing very large fractures is not inherently different from that governing moderate ones. The three largest stress reductions in the combined, untruncated distributions were also averaged to assess the relative contribution of high intensity fractures to cumulative fracturability.

#### Fractal and Fourier analysis

The fractal dimensions of the stress-strain functions were calculated using the Blanket Algorithm method described by Barrett et al. (1992), Normand and Peleg (1988), Peleg et al. (1984) and software written by Mark Normand (University of Massachusetts). Fractal dimension was determined for each of the six compression curve replicates and averaged.

Power spectra of the stress-strain functions were obtained using a Fast Fourier Transform algorithm from Systat. Parameters were obtained from the power spectra according to the procedure described by Barrett et al. (1994) and Rhode et al. (1993); spectra (obtained from the sum of the squares of the sine and cosine terms of the FFT) were averaged within specific frequency ranges and these values were averaged across replicates. The two frequency ranges used were 0.44–0.78 and 0.83–1.07 sec<sup>-1</sup>, respectively, corresponding to the 2nd and 3rd sixteenth sections of the power spectrum. Means were averaged across the six replicates.

## RESULTS

REPRESENTATIVE FRACTURE INTENSITY distributions for the 2% and 10% sucrose samples are shown (Fig. 2), illustrating how the number of fractures increased as fracture intensity decreased. However, the distributions were long-tailed, and showed the existence of a small number of fractures of very high magnitude. A substantial difference exists between the two plots since the distribution for the 10% sucrose samples was flatter and extended much further towards high magnitude fractures (plot does not show extremes of this distribution). By contrast, the bulk of the 2% sucrose distribution was in the low fracture magnitude range. While sucrose level influenced this difference in fracturability, the mechanism was possibly largely structural since high sucrose levels reduced expansion

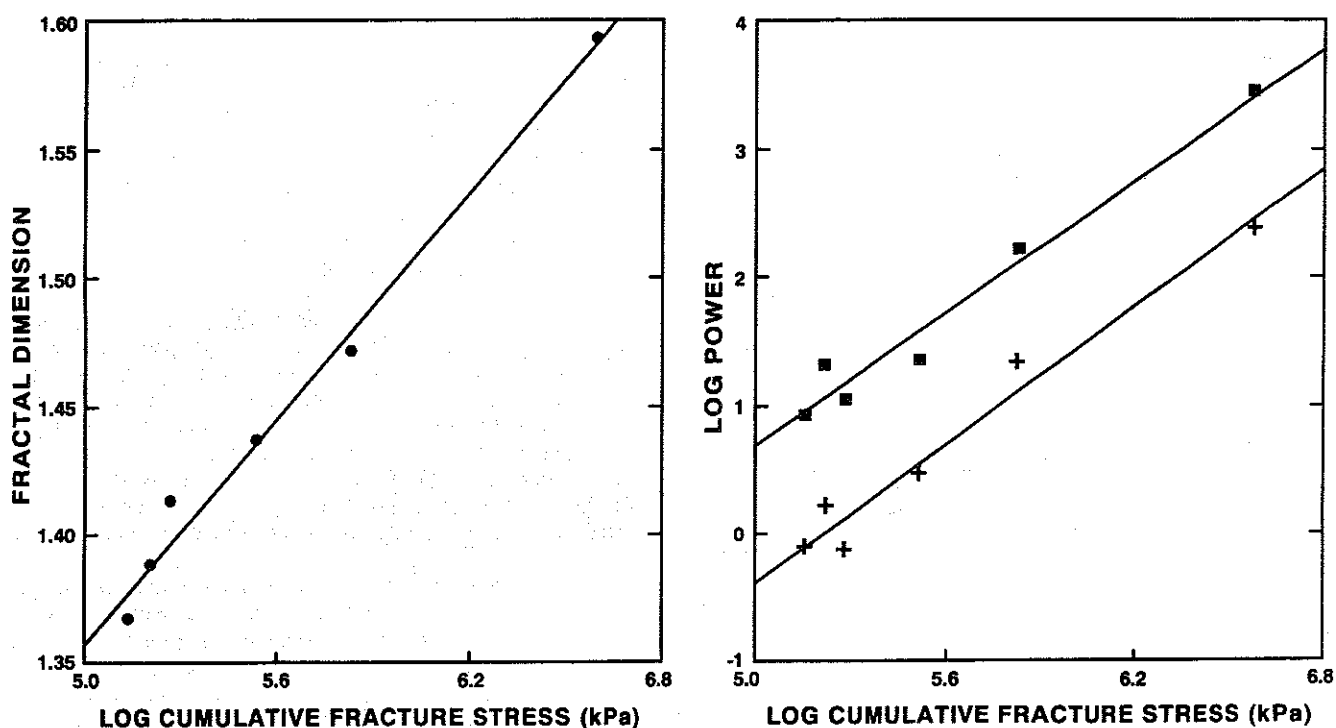


Fig. 3.—Relationship between log cumulative fracture stress and (a) fractal dimension, (b) log average power. ■ 1st frequency range; + 2nd frequency range.

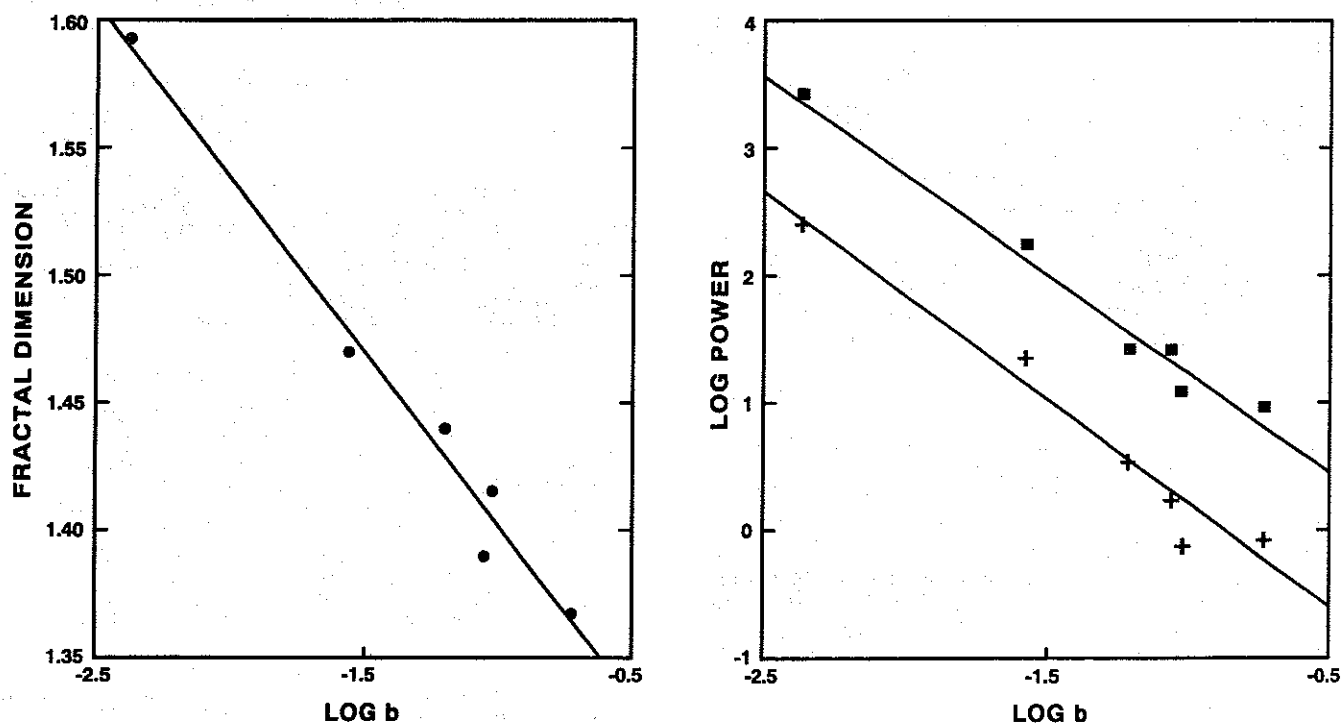


Fig. 4.—Relationship between log  $b$  and (a) fractal dimension, (b) log average power. ■ 1st frequency range; + 2nd frequency range.

(defined by extrudate cross sectional area/die cross sectional area, Table 1). Furthermore, cell sizes in the 6 sample lots appeared visually different.

The log of cumulative fracture stress is plotted against fractal dimension (which has theoretical limits of 1 and 2 for images) (Fig. 3a) and log average power in the two frequency ranges (Fig. 3b). Cumulative fracture stress correlated closely with either fractal dimension or average power, and correlation

coefficients for those relationships were respectively 0.98, 0.95 (first frequency range) and 0.96 (2nd frequency range).

Parameters from the fitted exponential distributions were compared (Table 1). Regression coefficients were in all cases between 0.86 and 0.95 except for the 10% sucrose sample, which had more scatter in the distribution ( $r^2=0.78$ ). The model exponent,  $b$ , is plotted against fractal dimension (semi-log plot) and average power (log-log plot, Fig. 4). Regression

**Table 2**—Extreme values of fracture intensity distributions and conformance to exponential model

Sucrose content (%)	n	Largest fracture intensity, kPa (in 6 replicates)	Average of 3 largest fracture intensities, kPa (in 6 replicates)	$\overline{L_u(n)} + 2\sigma_{L_u(n)}$
0	353	24.5*	18.8	25.5
2	368	27.5	22.8	18.4
4	329	27.9*	25.3	29.2
6	377	21.2*	17.8	24.9
8	413	45.6	35.5	43.8
10	430	62.3*	62.1	99.2

\* Within extreme value limit.

**Table 3**—Effect of relative humidity on cumulative fracturability

Sucrose content (%)	Freeze dried samples	Cumulative fracturability (kPa)	
		Equilibrated samples 43% RH	75% RH
0	184	32	9.6
2	173	34	22
4	252	64	32
6	194	58	19
8	342	68	26
10	723	168	16

coefficients for these relationships were respectively 0.98, 0.97 (first frequency range) and 0.95 (2nd frequency range).

Analysis of the largest stress reductions by extreme value theory showed that these fracture intensities in general conformed to the exponential model. Parameters of this analysis (Table 2) showed the largest fracture intensity, in the six replicates combined, was well within the extreme value limit of  $\overline{L_u(n)} + 2\sigma_{L_u(n)}$  in four cases (0,4,6, and 10% sucrose) and very close in a fifth (8% sucrose). For the remaining sample, the three largest fracture intensities were higher than the predicted value. However, those fractures occurred in only two of the sample replicates, and the remaining four were well within the extreme value limit for this distribution. The averages of the three largest fractures were also compared (Table 2). These values correlated generally with cumulative fracturability and were approximately equal to 10% of the cumulative fracturability.

Loss in fracturability due to moisture sorption was reflected in the cumulative fracturability measurements (Table 3). Reductions in cumulative fracture stress between 71 and 83% for samples equilibrated at 43% RH (yielding wet-basis moisture contents between 8.8 and 10.2%) and between 87 and 98% for those equilibrated at 75% RH (yielding wet-basis moisture contents between 10.9 and 11.8%). Distributions of fracture intensities were not fitted for these samples due to extreme losses in fracturability produced by equilibration. Furthermore, reductions in stress during compression of equilibrated samples were primarily of very low magnitude (> 80% smaller than 2 kPa for 43% RH samples; > 95% smaller than 2 kPa for 75% RH samples).

## DISCUSSION

FRACTURABILITY IN BRITTLE, puffed extrudates results from a multitude of individual fractures of varying magnitude. Fracture intensities form a distribution with a relatively greater number of low intensity fractures and proportionally fewer high intensity fractures. This distribution could be reasonably well described by an exponential function. A small number of very large fractures cause these distributions to be considerably long tailed. However, the highest intensity fractures can be shown to be consistent with the exponential distribution by

extreme value theory. That the distributions showed a range of fracture intensities was somewhat expected, given that the extrudate structures were nonuniform and also had wide distributions of cell sizes. Extrudate cell size distribution was described by right-skewed functions such as the log Normal and the Rosin-Rammler by Barrett and Peleg (1992); both functions accommodated the preponderance of smaller-sized cells observed from image analysis of the samples.

Fracturability parameters from fracture intensity distributions were related to those obtained through previously published fracturability-assessment techniques. Distribution exponents and cumulative fracturability correlated strongly with either the fractal dimension or power spectrum averages derived from stress-strain functions. Such a correlation was reasonable, given that each technique is based upon analysis of the oscillating behavior or "jagged" quality of the original function. An analogous correlation between fractal dimension and power spectrum averages was reported by Rhode et al. (1993). Furthermore, both fracturability parameters were related to structural characteristics and sensory texture by Barrett et al. (1994).

Quantification of fracturability by distribution analysis provides an alternative method to describe the texture of porous and brittle foods that can, furthermore, be applied using conventional statistical software. Parameters from this distribution can be used to quantify fracturability and to differentiate samples with different processing or storage histories. While use of an exponential function to describe fracture intensity distributions may be practically limited to reasonably brittle structures, cumulative fracture stress can be used to evaluate a wide range of samples that includes both brittle and nearly-plastic products.

## REFERENCES

- Barrett, A.H., Cardello, A.V., Leshner, L.L., and Taub, I.T. 1994. Cellularity, mechanical failure, and textural perception of corn meal extrudates. *J. Texture Studies* 25: 27.
- Barrett, A.H., Normand, M.D., Peleg, M., and Ross, E.W. 1992. Characterization of the jagged stress-strain relationships in puffed extrudates using the fast Fourier transform and fractal analysis. *J. Food Sci.* 57: 227.
- Barrett, A.H. and Peleg, M. 1992. Cell size distributions of puffed corn extrudates. *J. Food Sci.* 57: 146.
- Faubion, J.M. and Hosney, R.C. 1982. High-temperature short-time extrusion of wheat starch and flour. I. Effect of moisture and flour type on extrudate properties. *Cereal Chem.* 59: 529.
- Gumbel, E.J. 1958. *Statistics of Extremes*. Columbia University Press, New York.
- Halek, G.W., Paik, S.W., and Chang, K.L.B. 1989. The effect of moisture content on mechanical properties and texture profile parameters of corn meal extrudates. *J. Texture Studies* 20: 43.
- Hsieh, F., Peng, I.C., and Huft, H.E. 1990. Effect of salt, sugar and screw speed on processing and product variables of corn meal extrudated with a twin screw extruder. *J. Food Sci.* 55: 224.
- Lai, C.S., Guetzlaff, J., and Hosney, R.C. 1989. Role of sodium bicarbonate and trapped air in extrusion. *Cereal Chem.* 66: 69.
- Launey, B. and Lisch, J.M. 1983. Twin screw extrusion of starches: flow behavior in starch pastes, expansion and mechanical properties of extrudates. *J. Food Eng.* 2: 259.
- Normand, M.D. and Peleg, M. 1988. Evaluation of the "Blanket Algorithm" for ruggedness assessment. *Powder Technol.* 7: 255.
- Peleg, S., Naor, J., Hartley, R., and Avnir, D. 1984. Multiple resolution texture analysis and classification. *IEEE Transactions on Pattern Analysis and Machine Intelligence* 6: 4.
- Peleg, M. and Normand, M.D. 1992. Symmetrized dot-patterns (SDP) of irregular compressive stress-strain relationships. *J. Texture Studies* 4: 427.
- Rhode, F., Normand, M.D., and Peleg, M. 1993. Characterization of the power spectrum of force-deformation relationships of crunchy foods. *J. Texture Studies* 24: 45.
- Ryu, G.H., Neumann, P.E., and Walker, C.E. 1993. Effects of some baking ingredients on physical and structural properties of wheat flour extrudates. *Cereal Chem.* 70: 291.
- Smith, A.C. 1992. Studies on the physical structure of starch-based materials in the extrusion cooking process. In *Food Extrusion Science and Technology*. J. Kokini, C.T. Ho, and M.V. Karwe (Ed.) Marcel Dekker, Inc., New York.
- Sopade, P.A. and Le Grys, A. 1991. Effect of added sucrose on extrusion cooking of maize starch. *Food Control* 2: 103.

Ms received 12/9/93; revised 3/30/94; accepted 3/21/94.

We thank Jack Briggs of Natick for assistance in generating extrudate samples. We appreciate use of the Univ. of Massachusetts, Food Science Dept., computer facilities.